Biophysical Journal Volume 79 October 2000 1954–1966

Properties of Gap Junction Channels Formed by Cx46 Alone and in Combination with Cx50

Matthew G. Hopperstad, Miduturu Srinivas, and David C. Spray

Department of Neuroscience, Albert Einstein College of Medicine, Bronx, New York 10461 USA

ABSTRACT Gap junctions formed of connexin46 (Cx46) and connexin50 (Cx50) in lens fiber cells are crucial for maintaining lens transparency. We determined the functional properties of homotypic Cx46, heterotypic Cx46/Cx50, and heteromeric Cx46/Cx50 channels in a communication-deficient neuroblastoma (N2A) cell line, using dual whole-cell recordings. N2A cultures were stably and/or transiently transfected with Cx46, Cx50, and green fluorescent protein (EGFP). The macroscopic voltage sensitivity of homotypic Cx46 conformed to the two-state model (Boltzmann parameters: $G_{min} = 0.11$, $V_o = \pm 48.1$ mV, gating charge = 2). Cx46 single channels showed a main-state conductance of 140 ± 8 pS and multiple subconductance states ranging from ≤10 pS to 60 pS. Conservation of homotypic properties in heterotypic Cx46/Cx50 cell pairs allowed the determination of a positive relative gating polarity for the dominant gating mechanisms in Cx46 and Cx50. Observed gating properties were consistent with a second gating mechanism in Cx46 connexons. Moreover, rectification was observed in heterotypic cell pairs. Some cell pairs in cultures simultaneously transfected with Cx46 and Cx50 exhibited junctional properties not observed in other preparations, suggesting the formation of heteromeric channels. We conclude that different combinations of Cx46 and Cx50 within gap junction channels lead to unique biophysical properties.

INTRODUCTION

Gap junctions are pathways for intercellular communication through which small molecules and metabolites may pass. The channels that make up a junction are formed from the contribution of one hemichannel or connexon from each apposed cell surface. Hemichannels are themselves oligomers formed of six subunit proteins of largely α-helical structure (Unger et al., 1999; Bruzzone et al., 1996) called connexins. (Two nomenclatures for connexin types are in relatively common use, one using lowercase Greek letters that is based on closer similarity to archetypes (e.g., α_1 or β_1) and the other using the species and the molecular weight deduced from the cDNA clone (e.g., Cx32 or Cx43). We use the latter terminology in this report, where Cx46 and Cx50 correspond to α3 and α8 in the alternative nomenclature.) The channel properties of many of the known connexin isoforms have been characterized through electrophysiological inquiry by exogenous expression of the connexin type in mammalian cell lines and/or in the *Xenopus* oocyte system (for recent review see Verselis and Veenstra, 2000). These expression systems have also been used to elucidate the formation and functional properties of junctions that contain a different connexin type in each hemichannel (heterotypic) and of junctions that contain multiple connexin types in each hemichannel (heteromeric).

In this study we investigate the properties of channels formed by the two connexin types expressed in mammalian lens fiber cells, connexin46 (Cx46) (Paul et al., 1991) and connexin50 (Cx50) (White et al., 1992). Previous studies have shown that deletion of either of these connexins in mice leads to cataract formation (White et al., 1998; Gong et al., 1998). Moreover, coding region mutations in these genes lead to hereditary cataracts in humans and in mouse models (Shiels et al., 1998; Steele et al., 1997; Mackay et al., 1999). However, the specific roles of these connexins in the lens are not thoroughly understood. Intercellular communication in the lens via gap junctions has been proposed to be responsible for the transport of nutrients and metabolites (Goodenough., 1992; Mathias et al., 1997), as lens fiber cells lack direct access to blood supply. The properties of channels formed from Cx50, stably transfected in the same communication-deficient mouse neuroblastoma (N2A) cell line as used here, have previously been characterized as very high conductance and moderately sensitive to transjunctional voltage (Srinivas et al., 1999). Cx46 channels have previously been extensively characterized in the *Xenopus* oocyte system, where Cx46 is additionally capable of forming functional hemichannels (Ebihara and Steiner, 1993; Trexler et al., 1996; Paul et al., 1991; Pfahnl and Dahl, 1998).

In this study homotypic/homomeric Cx46 channels were characterized in N2A cell pairs transiently cotransfected with the cDNAs encoding rat Cx46 and enhanced green fluorescent protein (EGFP) contained in separate vectors. In addition, the possibilities of Cx46/Cx50 heterotypic and heteromeric channel formation were evaluated by coplating independent Cx46 and Cx50 transfected cells and by cotransfecting cells with both Cx46 and Cx50. The data from these preparations provides evidence for the physiological consequence of the simultaneous expression of these connexin types in the lens.

Received for publication 24 March 2000 and in final form 26 June 2000.

Address reprint requests to Dr. David C. Spray, Department of Neuroscience, Albert Einstein College of Medicine, 1300 Morris Park Ave., Bronx, NY 10461. Tel.: 718-430-2537; Fax: 718-430-8594; E-mail: spray@aecom.yu.edu.

0006-3495/00/10/1954/13 $2.00

MATERIALS AND METHODS

DNA construction and transfection

Rat Cx46 cDNA (generously provided by Dr. David L. Paul, Harvard Medical School, Boston, MA) was subcloned into pcDNA3 (Invitrogen, Carlsbad, CA) and pIRES (Clontech, Palo Alto, CA) expression vectors, and both were used. EGFP was obtained from Clontech in the expression vector. A fragment of genomic Cx50 corresponding to a full-length coding region (also provided by Dr. David L. Paul) was subcloned into pcDNA3. Most of the electrophysiological experiments described here were performed on N2A cells transiently transfected with connexin and EGFP cDNA. In some experiments, a stable Cx50 cell line was used (see Srinivas et al., 1999). N2A cells (obtained from ATCC, Rockville, MD) were transfected with the following amounts of DNA: Cx50 transfectants, 6 μg Cx50 DNA; Cx46/EGFP transfectants, 1.5–4.0 μg Cx46 DNA and 2.0 μg EGFP DNA; Cx46/Cx50/EGFP transfectants, 1.5–3.0 μg Cx46 DNA, 1.5–3.0 μg Cx50 DNA, and 2.0 μg EGFP DNA, using Lipofectamine Plus reagent (Gibco BRL, Gaithersburg, MD), following the procedure outlined by the manufacturer. Cell cultures were maintained in a 37°C incubator in a moist 5% CO_2/95% air environment.

To identify cell pairs in which each cell expressed a different connexin isoform, stable Cx50 transfectants were treated with 10 μM DiI C10 (a red fluorescent dye; Molecular Probes, Eugene, OR) for 1 h before freshly split cells were cocultured with those expressing either Cx46 and EGFP (heterotypic preparation) or Cx46, Cx50, and EGFP (heteromeric preparation). All cells were plated at low density on 1-cm glass coverslips; heterotypic and heteromeric cell pairs were identified via the difference in emission of EGFP (ex: 488 nm, em: >520 nm) and DiI C10 (ex: 540 nm, em: 575 nm), using a Nikon Diaphot microscope equipped with a xenon arc lamp and fluorescein isothiocyanate and rhodamine isothiocyanate filter sets. Faint double labeling was occasionally observed in these cultures (presumably because of cell debris or dye spread); only coupling between cells with pristine coloration was investigated.

Immunocytochemistry

Indirect immunofluorescence labeling of Cx46 in N2A-transfected cells and in mouse eye tissues (positive control) was carried out with slight modification of a procedure described previously (Dermeitzel et al., 1991). In brief, transfected cells and cryostat sections (8 μm) of the eyeballs of wild-type littermates were fixed on no. 1 glass coverslips with 3.7% formaldehyde for 10 min and permeabilized in 50% cold acetone for 2 min, 100% acetone for 5 min, and 50% acetone for 2 min, washed with Dulbecco's phosphate-buffered saline (PBS) (Gibco-BRL), and incubated in PBS supplemented with 0.5% bovine serum albumin (essentially globulin free; Sigma, St. Louis, MO) to block nonspecific labeling. The primary antibody used was anti-Cx46 mouse monoclonal IgG at 1:100 dilution in PBS (generously provided by Dr. Thomas Steinberg, Washington University School of Medicine, St. Louis, MO). The cells and sections were incubated with connexin antibody with preimmune antiserum overnight at 4°C. After extensive washing with PBS, coverslips were transferred to new culture dishes and exposed to Alexa 546-conjugated goat anti-rabbit IgG (Molecular Probes) at 1:2000 dilution at room temperature in the dark for 1 h. Coverslips were washed five times with PBS, then briefly with distilled water, and mounted on slides with the antifade reagent 0.1% paraphenylenediamine in a 10:1 mixture of 33% glycerol and PBS. The cells and specimens on the coverslips were viewed with a Nikon microscope equipped with fluorescein isothiocyanate excitation and emission filters and a mercury arc lamp. Nonspecific background staining was evaluated in adjacent eyeball sections and clonal N2A cells from which primary antibody had been omitted.

Electrophysiology

Coverslips were transferred to the stage of a Nikon Diaphot microscope and bathed in a external solution containing (in mM) 140 NaCl, 2 CsCl, 2 $CaCl_2$, 1 $MgCl_2$, 5 HEPES, 4 KCl, 5 dextrose, 2 pyruvate, and 1 $BaCl_2$ (pH 7.2). Junctional conductance was measured between cell pairs, using the dual whole-cell voltage-clamp technique with Axopatch 1C or 1D patch-clamp amplifiers (Axon Instruments, Foster City, CA). Each cell of a cell pair was voltage clamped with patch pipettes pulled on a Flaming/Brown Micropipette puller (model P-87; Sutter Instrument Co., Novato, CA). The patch electrodes had resistances of 3–8 MΩ when they were filled with internal solution containing (in mM): 130 CsCl, 10 EGTA, 0.5 $CaCl_2$, 3 MgATP, 2 Na_2ATP, and 10 HEPES (pH 7.2). All experiments were performed at room temperature. Macroscopic and single-channel recordings were filtered at 0.2–0.5 kHz and sampled at 1–2 kHz. Data were acquired using pCLAMP6 software (Axon Instruments); analysis was performed with pCLAMP6 and Origin 5.0 software (Microcal Software, Northampton, MA).

Each cell of a pair was initially held at a common holding potential of 0 mV. Voltage pulses of variable duration and amplitude were then applied to one cell to establish a transjunctional voltage gradient (V_j), and junctional current was measured in the second cell (held at 0 mV). The voltage sensitivity of gap junctions formed by homotypic Cx46 or Cx50 channels and heterotypic or heteromeric Cx46/Cx50 channels was studied using cell pairs that exhibited a total conductance of 2–7 nS to minimize the impact of series resistance on these measurements (Wilders and Jongsma, 1992). Junctional current was divided by the transjunctional voltage step to determine the macroscopic junctional conductance (g_j). To evaluate the voltage dependence of g_j, 7–10-s hyperpolarizing or depolarizing pulses were applied every 30 s from the holding potential of 0 mV to various test potentials ranging from −110 to 110 mV. Each voltage pulse was preceded by a −10-mV pulse of 50 ms duration. It was assumed that at this voltage all channels present in the junction were open and therefore conductance was at maximum. The instantaneous (I_{inst}) and steady-state (I_{ss}) levels of junctional currents were measured at the beginning and end of each voltage pulse. Instantaneous conductance (g_{inst}) was calculated for each voltage trace ($g_{inst} = I_{inst}/V_j$) and normalized to the conductance of the prepulse for each trace. These g_{inst} values were plotted as a function of V_j. Steady-state conductance (g_{ss}) at each voltage was normalized relative to g_{inst} and plotted as a function of V_j. The relationship between G_{ss} and V_j was fit assuming a two-state Boltzmann equation (Spray et al., 1981):

$$G_{ss} = \{(G_{max} - G_{min})/(1 + \exp[A(V_j - V_0)]\} + G_{min}$$

where V_0 is the voltage at which the voltage-sensitive component of g_j is half-maximal, G_{max} is the maximum normalized conductance, G_{min} is the normalized voltage-insensitive residual conductance, and A is a parameter defining the steepness of voltage sensitivity ($A = nqF$, where n is the equivalent number of gating charges of valence q and F is the Faraday constant).

Single-channel properties were investigated using pulse, ramp, and voltage reversal protocols as described in the figure legends. Gating events were recognized as simultaneously occurring events of equal amplitude and opposite polarity in current traces for both cells in the pair. All-points amplitude histograms of data were constructed for each experiment and fit to Gaussian functions to determine the mean and variance of the baseline and open-channel currents. Conductance histograms from single-channel ramp protocol records were constructed by dividing each digitized junctional current point by its corresponding nonzero V_j, plotting all points, and fitting each peak to a Gaussian function.

RESULTS

Cotransfection with EGFP predicts functional connexin expression

Electrical coupling was assessed in all transiently transfected Cx46 homotypic cells pairs 18–72 h after transfec-

tion. Maximum coupling, brightness of fluorescence, and percentage of fluorescing cells was observed ~48 h after transfection. A linear relation was observed between brightness of fluorescence (visually rated by each of the authors on an integer scale of 0 to 4 before patch clamping) and strength of electrical coupling measured in these pairs. Fig. 1 shows plots of log junction conductance for all cell pairs (Fig. 1 *A*) and mean junctional conductance (Fig. 1 *B*) versus fluorescence intensity ($n = 165$) recorded by the three investigators. This strong positive correlation between the magnitude of coupling and visual determination of fluorescence intensity greatly facilitated further studies, guiding the selection of cell pairs for macroscopic or single-channel recordings.

Expression of Cx46 protein was evaluated by immunocytochemical techniques using an anti-Cx46 antibody (Fig. 1, *inset*). In cells cotransfected with EGFP and Cx46, punctate Cx46 staining was clearly observed at appositional contacts between cells, suggesting that transfected N2A cells express Cx46 at the junction membrane. More importantly, staining for Cx46 was restricted to cells that contained EGFP, consistent with the strong correlation between EGFP fluorescence and coupling strength described above.

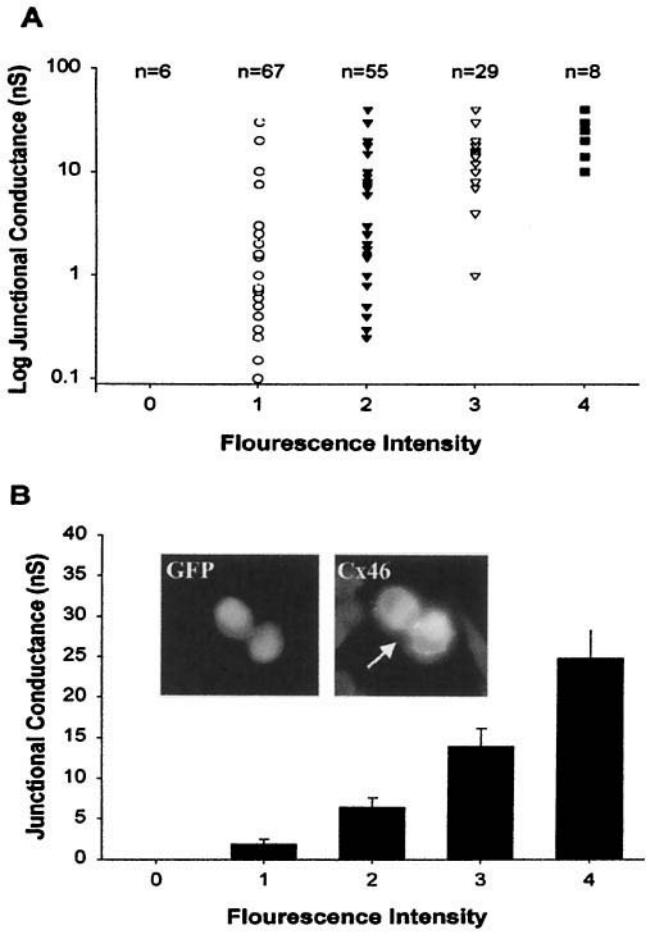

FIGURE 1 Functional expression of Cx46 and the relationship between junctional conductance and fluorescence intensity in otherwise communication-deficient N2A cells transiently cotransfected with rat Cx46 and EGFP cDNAs. Junctional conductance was measured in glowing cell pairs 24–72 h after transfection, using the dual whole-cell voltage-clamp technique. The brightness of fluorescence in each cell pair was visually assessed and was assigned a value on an integer scale of 0–4 (Fluorescence Intensity). (*A*) Semilogarithmic plot of junctional conductance as a function of fluorescence for all cell pairs tested (total $n = 165$). (*B*) Magnitude of electrical coupling is proportional to the fluorescence intensity. Junctional conductance values are indicated as means ± SEM of values shown in *A*. *B* (*Inset*) Immunocytochemical analysis of Cx46 expression in a EGFP fluorescing cell pair (*image at left*), detected using an anti-Cx46 antibody (*image at right*; Alexa 546-tagged secondary antibody). Punctate immunostaining was detected at appositions between cells (*arrow*).

Macroscopic properties of homotypic Cx46

The voltage sensitivity of gap junctions formed by multiple homotypic Cx46 channels was studied using cell pairs that exhibited a total conductance of 2–7 nS. Fig. 2 *A* shows a representative series of current traces from an N2A cell pair expressing Cx46 in response to a voltage step protocol in which one cell of the pair was held at 0 mV while the other cell was stepped from 0 mV to a series of voltages (−110 mV to +110 mV in 20-mV increments) for a duration of 8 s. Junctional currents in Cx46-transfected cells exhibited clear declines in a voltage- and time-dependent manner. These time- and voltage-dependent decreases in I_{ss} were clearly evident at $-20\ \text{mV} > V_j > 20\ \text{mV}$.

The dependence of the normalized steady-state conductance, G_{ss}, for homotypic Cx46 gap junction channels on the V_j is plotted in Fig. 2 *B* (*squares*). The voltage dependence of Cx46 gap junctions was assessed by assuming a two-state gating scheme and by using the Boltzmann equation (Materials and Methods) to fit G_{ss} values. The Boltzmann fits for the average G_{ss} values (from 10 cell pairs; SEM indicated for each G_{ss} value), shown as the solid lines in Fig. 2 *B*, are symmetrical around 0 mV. Boltzmann parameters are tabulated in Table 1.

Instantaneous currents of Cx50 gap junctions reportedly show no marked voltage sensitivity at high voltages of either polarity (Srinivas et al., 1999). However, Cx46 homotypic junctions show a clear decline in G_{inst} at $-80\ \text{mV} > V_j > 80\ \text{mV}$ with a reduction of ~20% at the largest depolarizing or hyperpolarizing voltages applied (±110 mV; Fig. 2 *B*, *triangles*).

Homotypic Cx46 channel properties

Characteristics of single-channel currents were determined from weakly fluorescing cell pairs cotransfected with Cx46 and EGFP. Fig. 3 illustrates characteristics commonly observed in single-channel currents for homotypic Cx46 junctions. The group of traces in Fig. 3 *A* represent the junctional current fluctuations in two cell pairs, each of which was coupled by a single Cx46 channel in response to 8-s

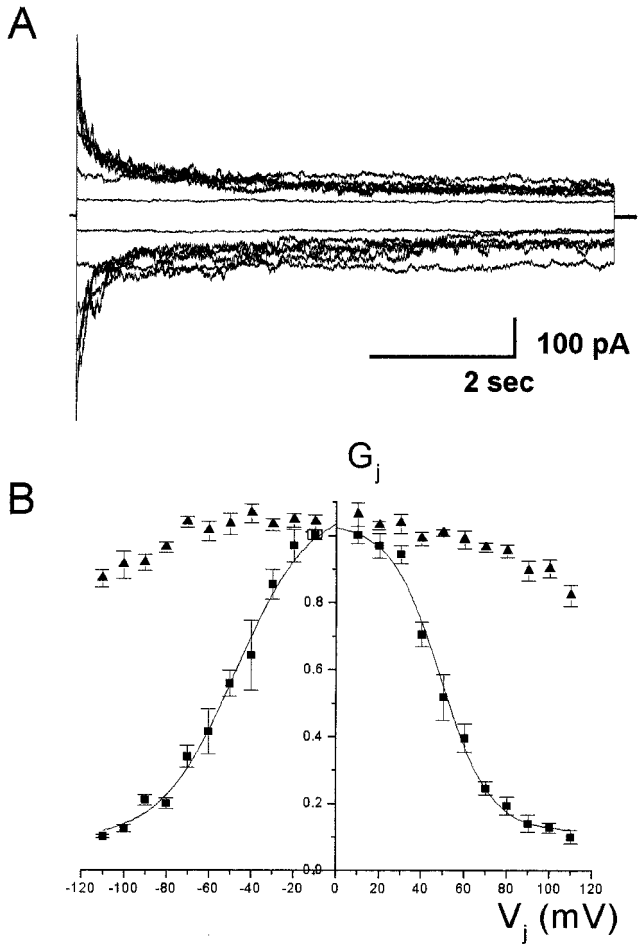

FIGURE 2 Dependence of junctional conductance of homomeric Cx46 gap junction channels on transjunctional voltage (V_j). (*A*) Recordings of junctional currents measured in one cell of a pair in response to 8–10-s-long pulses from 0 to ±110 mV in 20-mV increments that were applied to the other cell. Junctional currents were at maximum at the beginning of the pulses and declined to steady-state values in a time- and voltage-dependent manner when V_j exceeded ±20 mV. (*B*) Relationship of instantaneous and steady-state conductances to V_j in Cx46 gap junction channels. The normalized instantaneous (▲) and steady-state (■) junctional conductances at each voltage are shown; points represent the mean ± SE obtained for eight cell pairs, where $2 < g_j < 7$ nS. The solid line is a fit of the data to a two-state Boltzmann equation, with parameters corresponding to each quadrant indicated in Table 1.

voltage steps to −20, −40, −60, and −80 mV (one cell pair) and −100 mV (second cell pair) from a holding potential of 0 mV. The Gaussian fits to all-point histograms for each of the traces are shown to the right of each trace. For the single-channel currents at −20 mV and −40 mV, the amplitude histograms and Gaussian fits are additionally shown in Fig. 3 *B*, with peaks corresponding to 0 pA and 2.86 pA at 20 mV and 0 pA, 1.10 pA, and 5.82 pA at 40 mV. These peaks indicate a main-state conductance of ~145 pS and a residual subconductance state of ~27 pS. Such a residual subconductance state of ~25 pS was generally observed at V_j values beyond ±20 mV; in addition, residence in other subconductance states was observed as illustrated at the end of the −60 mV trace (where smaller subconductance states are not discretely resolved) and in the −80 mV trace (where the *dashed line* labeled S1 corresponds to a prolonged residence in a 52-pS substate). Fig. 4 shows single-channel current-voltage (*I-V*) relations from a third cell pair with one active channel in response to a 7.7-s ramp protocol that varied the applied voltage from −100 mV to 100 mV. The insets in this figure show all-points conductance histograms (see Materials and Methods) for the respective *I-V* relations as well as Gaussian fits. Peaks correspond to 0, 28, 55, and 155 pS (Fig. 4 *A, inset*) and 0, 28, 56, and 150 pS (Fig. 4 *B, inset*). The average main-state conductance (γ_j) of Cx46 channels measured from voltage ramps and pulses applied to junctions where a single channel was active was 140 ± 8 pS ($n = 8$).

TABLE 1 Boltzmann parameters for homotypic Cx46 and Cx50 and heterotypic Cx46/Cx50 channels

Parameter	Cx46	Cx50*	Cx46/50 (−)†	Cx46/50 (+)†
A	0.08	0.15	0.12	0.10
n	2.0	4	3.0	2.5
V_0 (mV)	48.1	37	43.1	42.3
G_{min}	0.11	0.22	0.26	0.07
G_{max}	1.06	1.00	1.01	1.02

*From Srinivas et al (1999).
†Refers to voltage polarity relative to the cell expressing Cx50.

For other connexins, macroscopic voltage sensitivity involves voltage-dependent transitions from the fully open state to a partially conducting residual conductance state (Bukauskas et al., 1995; Moreno et al., 1994; Srinivas et al., 1999). For Cx46 channels, the all-points histograms indicate the presence of multiple subconductance states ranging from ≤10 pS (the limit of resolution due to background noise) to 60 pS, although transjunctional voltage gradients appeared to primarily affect the distribution between the fully open and the ~25-pS conductance levels.

Cx46 channels appear to exhibit both fast and slow transitions from the open state to several subconductance states as well as to the fully closed state, in marked contrast to Cx50 channels. Examples of slow gating transitions of homotypic Cx46 channels are seen throughout Fig. 3, where specific examples are marked by arrowheads (−20 mV, −40 mV, and −60 mV). A particularly slow transition from a subconductance state to the fully closed state via what appears be a series of lower subconductance states is marked by the bar below the −60-mV trace. Transitions between multiple subconductance states may be responsible for the appearance of slow gating but remain indistinguishable from each other because of their low conductance (<10 pS), background noise (generally 1–2 pA when filtered during digitization at 200–500 Hz), and speed of digitization (1–1.5 kHz) of the analog signal. Furthermore, Cx46

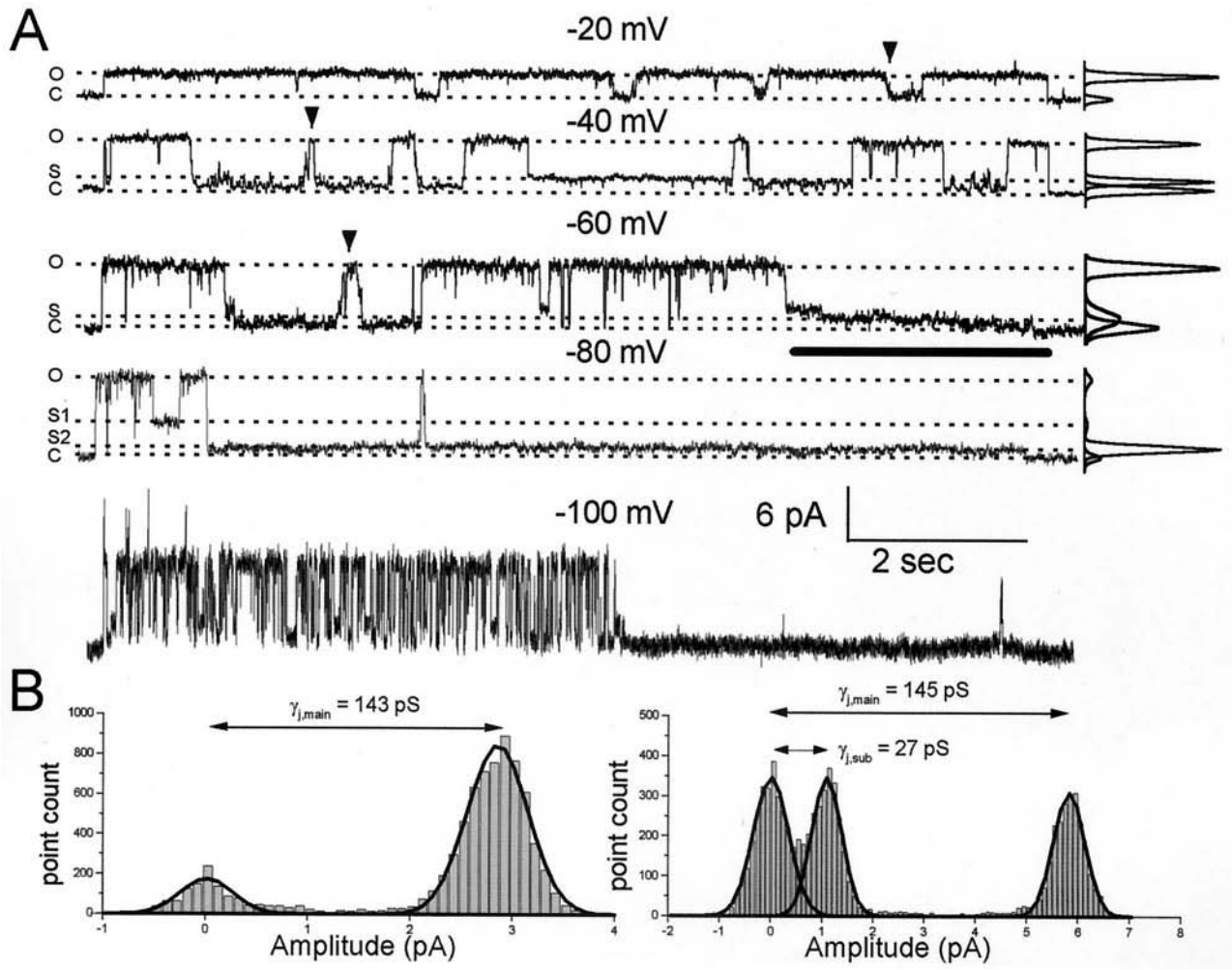

FIGURE 3 Gating properties of gap junction channels formed by Cx46 measured in cell pairs expressing one or two active channels. (*A*) Junctional currents in two Cx46-transfected N2A cell pairs in response to −20, −40, −60, and −80 mV (first cell pair) and −100 mV (second cell pair) from a holding potential of 0 mV. Single Cx46 channels were maximally open (O) from the baseline level (C) immediately upon application of a voltage pulse. Junctional current exhibited both fast and slow transitions to several subconductance states (S, S1, S2) and the closed state (C) from the fully open state (O). Slow transitions between the open state, subconductance states, and closed states (*arrowheads*) and between the closed state and several subconductance levels (*solid bar*) were often observed even in response to low V_j gradients. At high V_j Cx46 channels exhibited rapid gating (note in particular the −100 mV trace). Corresponding all-points amplitude histograms are shown to the right for all traces. (*B*) The all-points amplitude histograms and corresponding fits to Gaussian functions for current recordings obtained at V_j values of −20 (*left*) and −40 mV (*right*). The amplitude histogram at $V_j = -20$ mV has two peaks at 0 pA and 2.86 pA corresponding to a conductance of 143 pS for the fully open state. At $V_j = -40$ mV, three peaks at 0 pA, 1.08 pA, and 5.82 pA were observed, corresponding to the closed state, a subconducting state ($\gamma_{j,sub} = 27$ pS), and the fully open state ($\gamma_{j,main} = 145$ pS), respectively.

channels often exhibited distinctive gating characteristics at high transjunctional voltages, as shown in Fig. 3 (−100 mV): main-state to subconductance or closed-state transitions were regularly composed of relatively long bursts of rapid gating characterized by short dwell times in the open, subconductance, or closed states.

Macroscopic properties of heterotypic Cx46/Cx50 junctions

To determine whether Cx46 and Cx50 formed functional heterotypic channels, cells transiently expressing Cx46 were paired with those stably expressing Cx50, as described in Materials and Methods. Fig. 5 *A* shows a representative series of current traces from a heterotypic Cx46/Cx50 cell pair in response to a pulse protocol where the cell expressing Cx50 was pulsed to a series of voltages ranging from −110 mV to 110 mV in 10-mV steps. The junctional current shown was recorded from the cell expressing Cx46, and normalized junctional conductance (G_j) is plotted in Fig. 5 *B* with reference to pulse magnitude and polarity applied to the cell expressing Cx50 (V_{j50} on *abscissa*). The G_j-V_j relationship ($n = 7$ with SEM indicated for all normalized g_j values) shows a clear, ~20% rectification in the

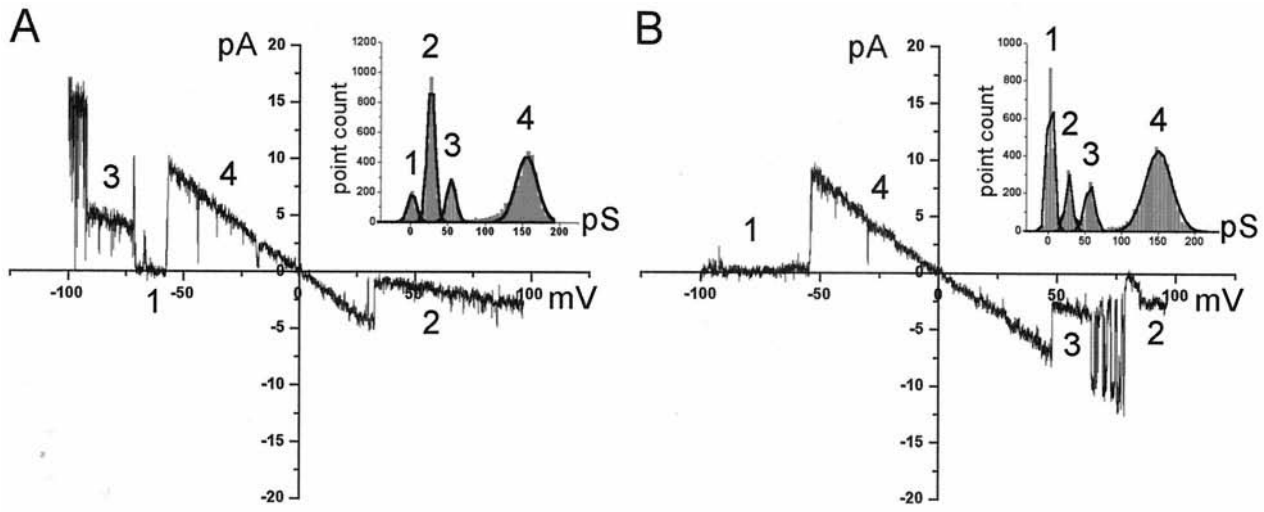

FIGURE 4 Single-channel current-voltage (I_j-V_j) relationships of the junctional current constructed from the responses of a Cx46-expressing cell to a series of ramps from −100 to +100 mV. The unitary conductances of the main state and the several subconductance states were measured by constructing conductance histograms (*insets*) for all data points at nonzero V_j. Numbers (1, 2, 3, 4) show the correspondence between peaks in each histogram and specific conductance states in the *I-V* relation. Peaks from left to right in histograms are 0, 28, 55, and 155 pS (*A inset*) and 0, 28, 56, and 150 pS (*B inset*).

instantaneous conductance from ±110 mV (*triangles*); lowest and highest values were found when the highest transjunctional voltage applied was negative (−110 mV) and positive (110 mV) relative to the Cx50 expressing cell pair, respectively. The Boltzmann fit to the steady-state G_j-V_j data (*solid line*) indicates significant differences in Boltzmann parameters for the constituent hemichannels in the heterotypic preparation when compared with either homotypic channel type (see Fig. 2 and Table 1). The clear presence of voltage-dependent reductions in junctional currents for pulses of either polarity suggests that the constituent hemichannels share the same relative transjunctional gating polarity. Assuming a positive relative transjunctional voltage gating polarity for both Cx46 and Cx50 (see Discussion), G_{min} values were significantly reduced in the Cx50-expressing cell pair (positive V_{j50} values) and concomitantly increased in the Cx46-expressing cell pair (negative V_{j50} values) when compared with values in homotypic Cx50 and Cx46 channels.

Single-channel properties of heterotypic Cx46, Cx50 junctions

Fig. 6 illustrates single-channel gating properties of heterotypic Cx46/Cx50 channels. Fig. 6 *A* shows an ensemble *I-V* relationship (*left*) for seven traces, using a ramp protocol that varied the applied voltage from −100 mV to 100 mV over the course of 7.7 s (illustrated in the *inset*). The cell expressing Cx50 was pulsed, and current was recorded from the cell expressing Cx46; as in Fig. 5, transjunctional voltages are plotted with regard to the polarity in the Cx50-expressing cell (illustrated in the *inset* in Fig. 6 *A*). The *I-V* relation of one of the seven traces is shown to the right for clarity. Currents shown in Fig. 6 *B* were elicited from a single cell pair with a 10-s protocol in which the cell expressing Cx50 was pulsed to the voltage shown and then voltage was reversed to the opposite polarity but the same magnitude (applied voltage waveforms are shown above each corresponding current trace in Fig. 6 *B*). Similar but inverted voltage gating properties were observed in records in which the cell expressing Cx46 was pulsed and junctional currents were recorded in the Cx50-expressing cell.

The ramp protocol shown in Fig. 6 *A* illustrates clear deviations from linearity in the main-state current-voltage relationship for heterotypic Cx46/Cx50 channels. Increasing depolarization of the cell expressing Cx46 (data not shown) or hyperpolarization of the cell expressing Cx50 resulted in a clear decline in main-state conductance from ~165 pS at V_{j50} = −10 mV to ~140 pS at V_{j50} = −100 mV. Conversely, hyperpolarization of the cell expressing Cx46 (data not shown) or depolarization of the cell expressing Cx50 resulted in a significantly increasing γ_j with increasing hyperpolarization (maximum γ_j ~210 pS at V_{j50} = 100 mV). Rectification of main-state conductance was consistently observed in currents elicited from both pulse and ramp protocols, although some variation in the degree of rectification was observed from one experiment to the next. Subconductance state rectification was difficult to assess because of the conservation in heterotypic channels of the multiple subconductance states observed in homotypic Cx46 channels. Fig. 6 *B* (in particular, the current traces at −100 mV) show the presence of multiple conductance states attributable to gating of the Cx46 hemichannel: at −100 mV incomplete channel opening is followed by

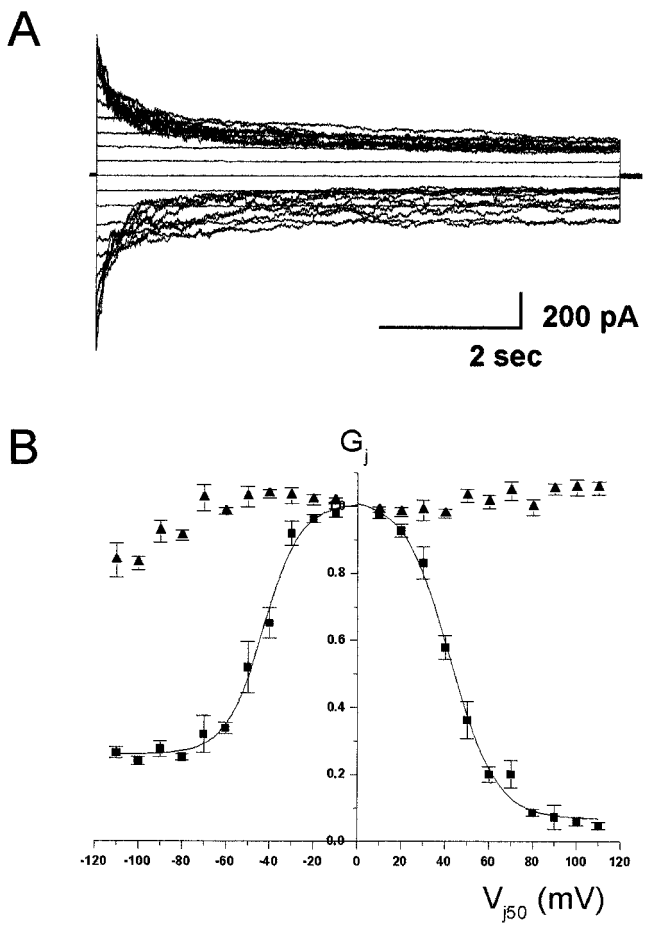

FIGURE 5 Dependence of junctional conductance of heterotypic Cx46-Cx50 channels on transjunctional voltage (V_j relative to the Cx50-expressing cell is plotted and is indicated as V_{j50}). (*A*) Recordings of junctional current measured in the Cx46-expressing cell in response to 8–10-s-long pulses from 0 to ±110 mV in 10-mV increments that were applied to the Cx50-expressing cell. Junctional currents declined to steady-state values in a time- and voltage-dependent manner when V_j exceeded ±20 mV. Note that the instantaneous current exhibits significant rectification: magnitudes of the currents were largest when high positive V_j values and smallest when high negative V_j values were applied to the Cx50-expressing cell of the pair. (*B*) The relationship between the normalized instantaneous (▲) and steady-state (■) junctional conductances and V_j (relative to the cell expressing Cx50), illustrating rectification of the instantaneous conductance and the dependence of G_{min} on relative V_j. Points represent the mean ± SE obtained in seven experiments. The solid line superimposed on the steady-state data is a fit of the data to a two-state Boltzmann equation. Boltzmann parameters are shown in Table 1. Properties observed in heterotypic junctions are significantly different from those expected if independence is assumed for the constituent hemichannels. Compare Boltzmann parameters of homotypic and heterotypic channels in Table 1.

brief sojourns in at least three distinct subconductance states (*arrowheads*). Also illustrated in these traces are main-state rectification (γ_j = 185 pS at 60 mV and γ_j = 160 pS after the voltage is reversed to −60 mV) and the indication that the lower g_{min} values observed in macroscopic recordings are attributable both to the presence of a lower residual conductance at positive V_{j50} values and to sojourns to a fully closed state (Fig. 6 *B*, 100 mV, 70 mV, and 60 mV).

To compare single-channel gating properties of heterotypic channels with those of homotypic Cx50 (reported by Srinivas et al., 1999) and Cx46 channels, longer recordings were compared from cell pairs exhibiting a single active channel of each type. Fig. 7 shows junctional currents from a homotypic Cx46 channel in response to a −40-mV pulse (Fig. 7 *A*) and a heterotypic channel in response to 40 mV (Fig. 7 *B*) and −40 mV (Fig. 7 *C*) pulses applied to the cell expressing Cx46. The top panels in Fig. 7, *A–C*, have durations of 40, 38, and 30 s, respectively; lower traces in each panel are 5-s segments on an expanded time scale corresponding to the bar beneath each upper trace. Arrowheads in Fig. 7, *B* and *C*, indicate the application of the voltage pulse; the asterisk in Fig. 7 *C* indicates termination of the voltage pulse. At −40 mV the homotypic Cx46 channel exhibited transitions between a very low subconductance or closed state and the main state (Fig. 7 *A*, γ_j = 142 pS (O)); both fast and slow gating transitions were observed, as indicated in the expanded segments of the recording. For the heterotypic channel, application of a −40-mV transjunctional voltage relative to Cx50 (Fig. 7 *B*) resulted in channel activity predominantly composed of fast transitions between the main state (γ_j = 163 pS (O)) and a relatively large-amplitude subconductance state ($\gamma_{j,sub}$ = 65 pS (S)) with additional transitions to multiple subconductance states. Application of a 40-mV pulse to the Cx50 side of this heterotypic channel (Fig. 7 *C*) resulted in brief channel activity (γ_j = 170 pS (O)), including a clear incidence of slow gating (indicated in the expanded segment), before relatively stable channel residence in a low subconductance state ($\gamma_{j,sub}$ = 27 pS (S)).

Heteromeric channel formation

To determine whether Cx46 and Cx50 formed functional heteromeric channels, we cotransfected N2A cells with Cx46 and Cx50 and compared the properties of junctional currents in these cells with those obtained for homotypic Cx46 and Cx50 and heterotypic Cx46/Cx50 channels. Initially, both macroscopic and single- or multichannel currents were measured (n = 60 cell pairs). Macroscopic voltage sensitivity of such cotransfectants (data not shown) was not demonstrably different from the conductance of channels formed by either homotypic or heterotypic combinations as illustrated in Figs. 2 and 5, which we attribute to the similarities in macroscopic gating properties of homotypic Cx46 and Cx50 junctions and the perturbation in these gating characteristics introduced by heterotypic channel formation (see Table 1). Evidence that heteromerization might be present in the cotransfected cells was provided in multichannel recordings, where several discrete amplitudes of current were observed, corresponding to unitary conductances between 100 pS and 190 pS (Fig. 8, *A* and *B*). To

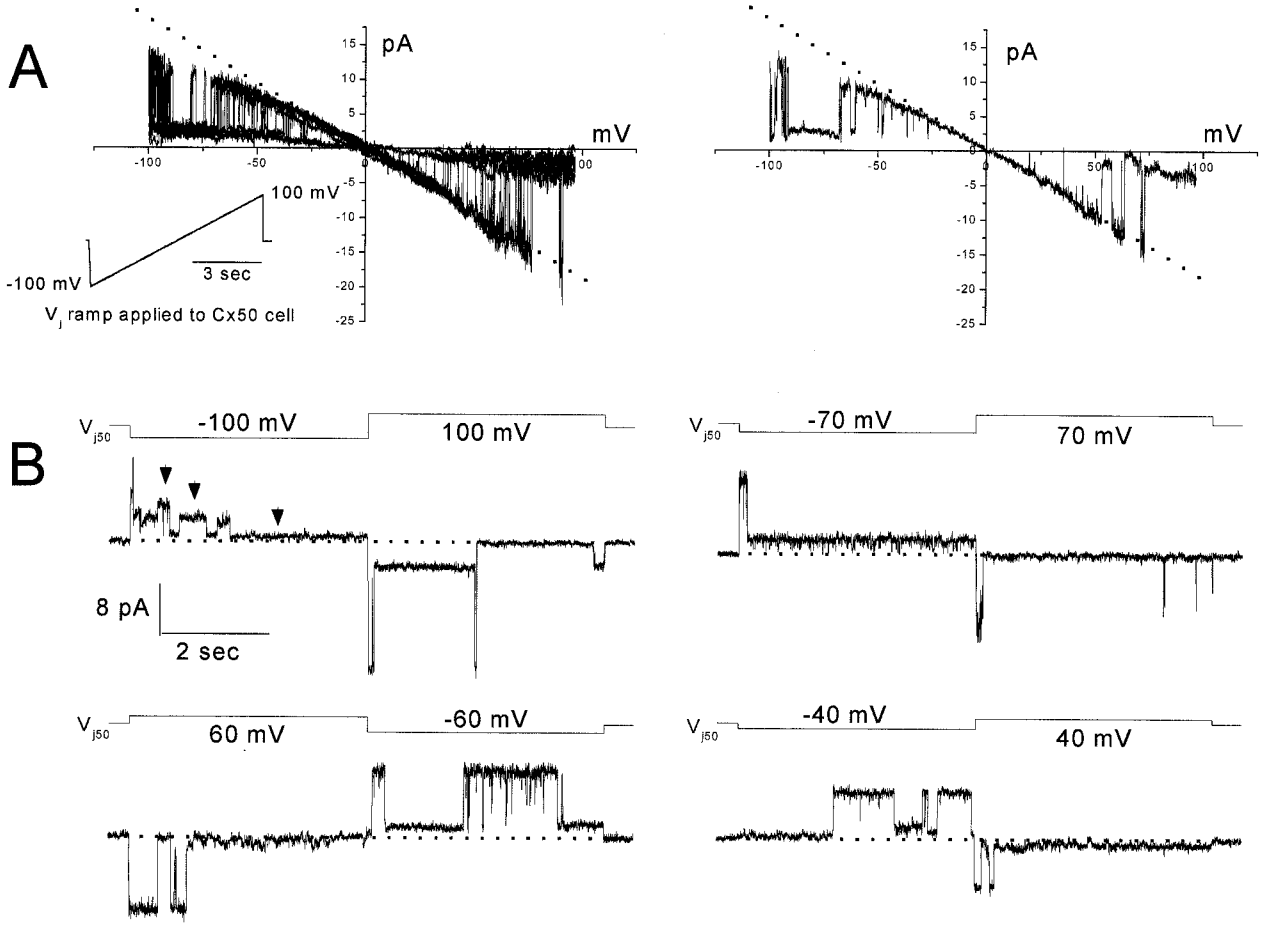

FIGURE 6 Single-channel properties of heterotypic Cx46-Cx50 channels illustrating rectification of the main-state conductance. (*A*) Single-channel currents in response to a series of ramps from −100 to +100 mV applied to the Cx50-expressing cell; one trace is displayed alone for clarity to the right. The single-channel current displays significant rectification; conductance is lowest (140 pS) at $V_j = -100$ mV and highest (210 pS) at $V_j = 100$ mV. The slope conductance (*dashed line*) measured between −10 and +10 mV was 165 pS. (*B*) Single-channel currents elicited from a single cell pair with a 10-s protocol in which the cell expressing Cx50 was first pulsed to the voltage shown and then the voltage was reversed to the opposite polarity at equal amplitude (corresponding voltage waveforms are illustrated above each trace). Note that the main-state current was higher when the Cx50 cell pair was made positive (e.g., $\gamma_j = 185$ pS at 60 mV and $\gamma_j = 160$ pS after the voltage was reversed to −60 mV), suggesting that both Cx46 and Cx50 gate at positive voltages. Arrowheads in −100-mV trace signify the presence of multiple subconductance states when V_j relative to the Cx50-expressing cell was negative.

pursue this issue further, and to reduce the ambiguity of multiple subconductance states with multiple channel types, we have analyzed in detail recordings from cotransfectants in which a single channel was active. Of the 10 such recordings obtained, the properties of most were not demonstrably different from those obtained for either homotypic or heterotypic channels. However, in a small number of cases ($n = 3$), cotransfection led to recordings of single-channel currents with intermediate properties between those of homotypic or heterotypic Cx46 and Cx50 channels. Distinct examples of such intermediate single-channel properties are shown Fig. 8, *C* and *D*, for two of these cell pairs in response to ramp protocols. In the first case, main-state conductance was 134 pS, a value slightly lower than that of Cx46 homotypic channels; transitions of these channels from the open state to subconductance states were in most cases rapid like those of Cx50 channels and unlike those found for homotypic Cx46 channels. In the second example, single-channel conductance was 160 pS (measured between −20 and 20 mV), a value similar to that seen in Cx46/Cx50 heterotypic pairings; however, in contrast to single-channel currents of heterotypic Cx46/Cx50 channels, rectification of main-state currents was only moderate, ranging from 140 pS at −100 mV to 175 pS at 100 mV (compare to Fig. 5 *A*, where conductance varied from 140 pS to 210 pS between these V_j values).

DISCUSSION

Gap junction channels are formed by the pairing of hexameric connexins or hemichannels contributed by each cell. Connexins 50 and 46 are coexpressed in lens fiber cells,

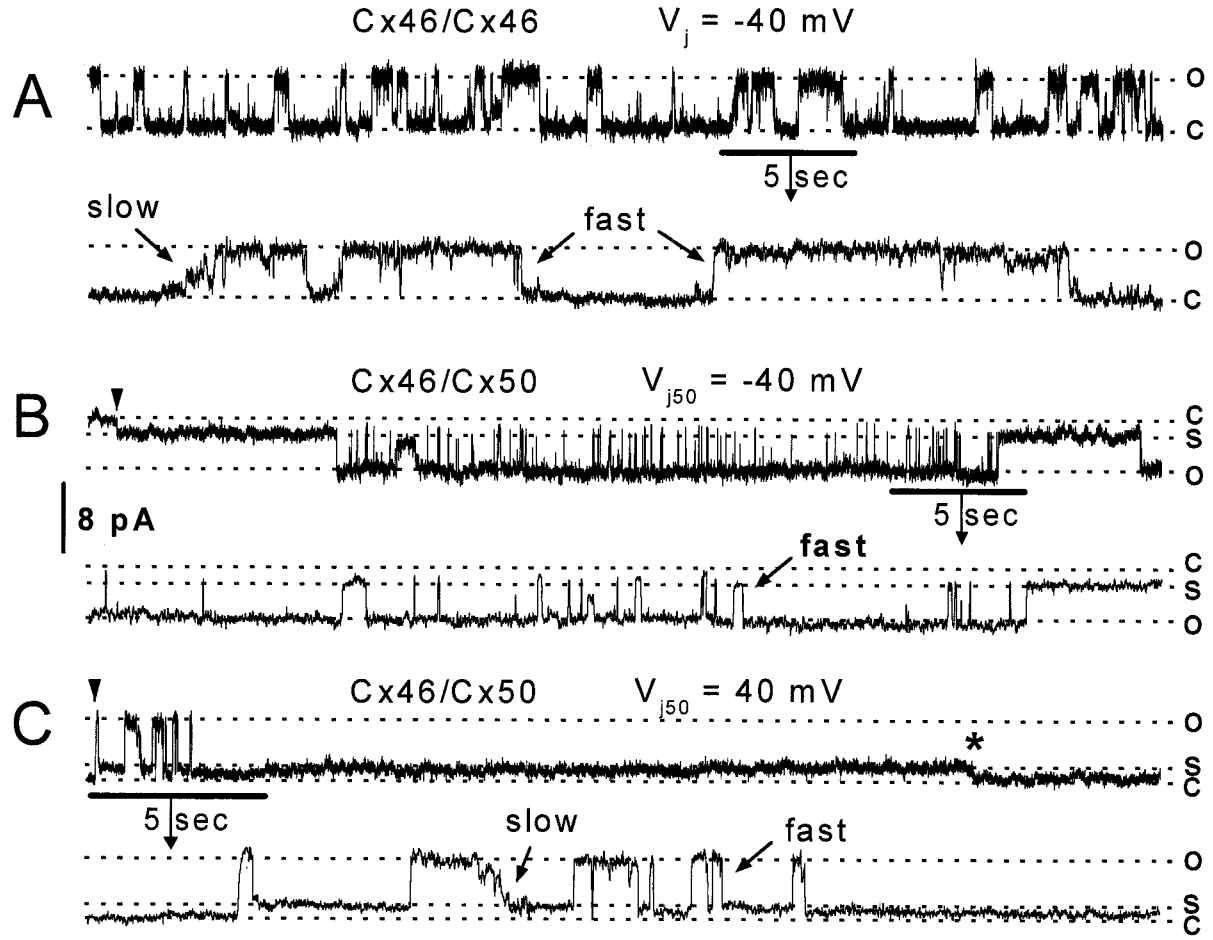

FIGURE 7 Heterotypic pairing of Cx46 with Cx50 leads to marked changes in the gating behavior of the constituent hemichannels. Single-channel records in response to long V_j pulses in homotypic Cx46 junctions at $V_j = -40$ mV (*A*) and Cx46/Cx50 junctions at -40 mV (*B*) and 40 mV (*C*). The top traces in *A*, *B*, and *C* represent a slow time scale, which is amplified ~10-fold in the traces below, although the V_j polarity is indicated relative to the Cx50 cell, to be consistent with other figures. (*A*) In the heterotypic junction, pulses were applied to the Cx46-expressing cell. In homotypic Cx46 junctions, transitions occurred between the open, closed, and several intermediate conductance states. Both fast and slow transitions were observed as indicated. (*B*) Gating attributed to the Cx46 side of heterotypic Cx46/Cx50 junctions, evident in single-channel records at $V_{j,50} = -40$ mV, was predominantly composed of fast transitions between the main state and subconductance states. (*C*) At $V_{j,50} = 40$ mV, channel activity was composed of both fast and slow transitions, similar to the behavior of homotypic Cx46/Cx46 channels. Bars beneath the top trace in each panel represent the 5-s segment shown on an expanded time scale in the lower trace. Arrowheads in *B* and *C* indicate initiation of the voltage pulse. The asterisk in *C* indicates termination of the pulse.

raising the possibility that gap junction channels between these cells might be homomeric (formed exclusively by multiple copies of either of these connexins), heterotypic (formed by the pairing of homomeric Cx46 and Cx50 connexons), or heteromeric (with both connexins expressed within a connexon). We previously described the properties of Cx50 homomeric channels stably expressed in communication-deficient mammalian cells (Srinivas et al., 1999) and now report results from experiments characterizing channels formed by Cx46 homomers, Cx46 homomers paired with Cx50 homomers, and channels where each cell was cotransfected with both connexins. All combinations of the lens fiber connexins exhibited moderately voltage-sensitive junctional conductance and displayed unitary conductances higher than those of most connexin types previously characterized (for a recent review, see Verselis and Veenstra, 2000). However, data from heterotypic and possibly heteromeric channels revealed deviations from that expected from homomeric recordings, consistent with the complex gating behavior previously reported for Cx46 hemichannels.

Transient cotransfection with a visible marker

The experiments described here demonstrate that simultaneous transient transfection with expression vectors containing EGFP and connexin coding sequences can be used to predict the extent of functional connexin expression via the brightness of fluorescence. Such a method tremendously

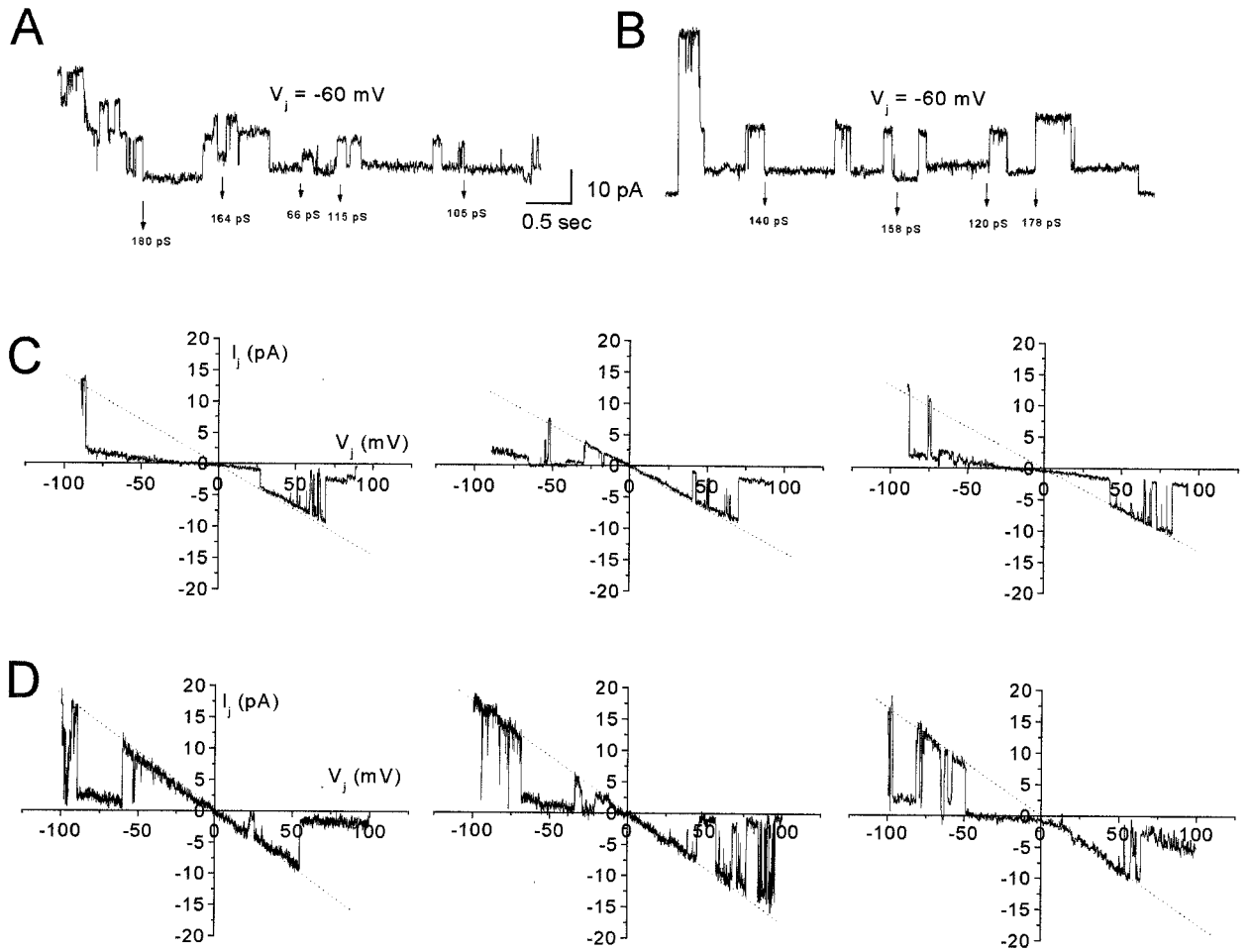

FIGURE 8 Possible evidence for the formation of heteromeric Cx46/Cx50 channels in cells transfected with both Cx46 and Cx50. (*A* and *B*) Multichannel currents in response to a −60 mV pulse from two different cell pairs, showing multiple transition sizes, as indicated between 66 pS and 180 pS. Similar transitions were consistently observed in homotypic and heterotypic Cx46 and Cx50 channels. (*C*) Single-channel currents in response to a series of three ramps from −90 to +90 mV. The single-channel conductance, measured as the slope conductance between ± 20 mV, is 134 pS. Some degree of rectification can be detected. However, despite the low unitary conductance, gating appears to be qualitatively similar to that of homotypic Cx50 channels. (*D*) Single-channel currents in response to a series of three ramps from −100 to +100 mV. Single-channel conductance is 160 pS with moderate rectification.

accelerates the generation of starting materials when compared to the establishment of stable transfectants and optimizes the selection of poorly coupled cells for single-channel studies. Our use of this technique in studies of other wild-type and mutant connexins in the N2A cell line has indicated a similar relationship between fluorescence and coupling levels, although the optimal DNA concentration varies considerably for each of the various connexin types (unpublished observations). Presumably the linear relationship observed between the brightness of EGFP fluorescence and junctional conductance is due to proportionality in the efficacy of intercellular incorporation of the EGFP and connexin vectors during transfection for each cell. Cotransfection of other connexins with EGFP yielded channels with properties that were identical to those in stable cell lines, demonstrating that coexpression of EGFP does not measurably alter the properties of channels.

Homotypic Cx46 channels: comparison to Cx50 channels and Cx46 hemichannels

We previously reported that homomeric channels formed by Cx50 in stably transfected N2A cells were moderately voltage dependent, and the voltage-sensitive component of steady-state junctional conductance (G_{ss}) was fit well by a two-state Boltzmann relation, as are other gap junction channel types ($V_0 = 37$ mV, $G_{min} = 0.22$, $A = 0.15$, $n = 4$; Srinivas et al., 1999). Instantaneous g_j in Cx50 pairs was unaffected by transjunctional voltage (V_j). Single-channel

currents through Cx50 channels exhibited rapid voltage-dependent transitions from a main-state conductance of 220 pS to a single residual conductance state of 43 pS, where the main-state open probability determined the voltage-dependent component of steady-state junctional conductance. Very similar values for macroscopic and unitary conductance properties were obtained in studies of N2A cell pairs transiently cotransfected with Cx50 and EGFP vectors (not illustrated), demonstrating that transient transfection yields channels with properties virtually identical to those of stable expression and that the coexpression of EGFP did not measurably alter those properties.

The studies described here characterizing Cx46 homomers show distinctive properties compared to those of the other lens fiber connexin. Using cell pairs in which junctional conductance was <7 nS, to avoid errors due to series resistance (see Wilders and Jongsma., 1992), we again found that the data fit reasonably well fit to a moderately voltage-sensitive two-state Boltzmann relation, although parameters differed from those of Cx50 ($V_0 = 48.1$ mV, $G_{min} = 0.11$, $A = 0.08$). In contrast to Cx50, however, instantaneous conductance of Cx46 channels was markedly decreased at 80 mV $< V_j <$ −80 mV; thus, at $V_j = 100$ mV, the G_{inst} value was 90 ± 5% of that measured at ±20 mV. Boltzmann parameters obtained in this study differ from those obtained for Cx46 gap junction channels expressed in oocytes (White et al., 1994b); whether these differences are due to differences in posttranslational processing remains to be determined.

Unitary junctional currents were resolved in both multichannel and single-channel recordings from Cx46-expressing cell pairs without the use of uncoupling agents or de novo pairing protocols (e.g., Burt and Spray, 1989; Bukauskas and Weingart, 1994; Bukauskas et al., 1995). These studies revealed that Cx46 channels expressed in mammalian cells possessed a main-state conductance of 140 ± 8 pS and multiple subconductance states ranging from ≤10 pS to 60 pS, with a predominate state of ~25 pS. In contrast to channels formed by Cx50, transitions between states (open, subconductance, and closed) could be either rapid ("fast") or prolonged ("slow"). Transitions could require tens of milliseconds for completion, during which channels might reside in multiple additional partially conducting states. Slow transitions of junctional channels between conducting states were initially described in pairs of chick heart cells (Veenstra and DeHaan, 1988) and subsequently characterized in detailed studies of newly paired insect and mammalian cell types where such events were associated with channel formation or docking of adjacent connexons (Bukauskas and Weingart, 1994; Bukauskas et al., 1995).

Previously, Cx46 channels have been extensively studied in the *Xenopus* oocyte expression system (White et al., 1994b), where Cx46 is additionally capable of forming functional hemichannels (Ebihara and Steiner, 1993; Trexler et al., 1996; Paul et al., 1991; Pfahnl and Dahl, 1998). The macroscopic voltage sensitivity of Cx46 hemichannels is biphasic, with conductance increasing at potentials higher than −20 mV (Ebihara and Steiner., 1993) and decreasing beyond 60 mV (Trexler et al., 1996). Such behavior was first interpreted as indicating that heterotypic pairing induces allosteric change in the Cx46 hemichannel, leading to a change in the relative transjunctional gating polarity (White et al., 1994a), but a later report (Trexler et al., 1996) showed that Cx46 hemichannels possess two voltage-sensitive gates, each sensing an opposite polarity. These single-channel studies on Cx46 hemichannels in oocytes demonstrated that application of depolarizing pulses led to fast transitions between the open state and a subconductance state, while application of hyperpolarizing pulses led to slow transitions that were attributed to the presence of a second gate with an opposite polarity of voltage sensitivity (the so-called loop gate (Trexler et al., 1996); also termed the p_o gate (Pfahnl and Dahl, 1998)). The presence of both fast and slow transitions in our cell-cell channel recordings, as well as the asymmetrical gating properties of heterotypic Cx46/Cx50 channels (see below), are consistent with the presence of dual gates in each Cx46 hemichannel, although alternative explanations involving conformational differences between channels and hemichannels cannot be ruled out (see below). The unitary conductance of Cx46 cell-to-cell channels ($\gamma_j = 140 \pm 8$ pS) measured while applying low to moderate transjunctional voltage gradients was consistent with the approximate Ohmic sum of resistances of constituent hemichannels (unitary conductance (γ_{hj}) ≈ 300 pS; Trexler et al., 1996; Pfahnl and Dahl, 1998).

Heterotypic Cx46/Cx50 channels

Macroscopic voltage dependence of steady-state g_j in heterotypic Cx46/Cx50 pairs was asymmetrical, with pulses of positive polarity applied to either the Cx46 or Cx50 cell, yielding voltage sensitivities that differed from either homotypic junction type (see Table 1). Instantaneous junctional conductance was also asymmetrical, being lowest at large positive transjunctional voltages relative to the Cx46 side.

Measurements of single-channel properties provided evidence for a positive relative transjunctional gating polarity for both Cx46 and Cx50. Single-channel conductance was similar to that of homotypic Cx50 (~210 pS) when V_j was positive relative to the Cx50 expressing cell and was similar to that of Cx46 (~140 pS) when V_j was positive relative to the cell expressing Cx46. In addition, the multiple subconductance states and bursts of rapid gating (at −80 mV $> V_j >$ 80 mV) observed in homotypic junctions were also observed in heterotypic junctions when similar transjunctional voltages were positive relative to the cell expressing Cx46. The conservation of these properties leads us to conclude that the primary gates in both Cx46 and Cx50 that are responsible for the macroscopic current declines close in

response to positive relative transjunctional voltages (see Verselis et al., 1994).

Rectification of instantaneous conductance similar to that observed here was also observed in Cx26/Cx32 heterotypic channels (Suchyna et al., 1999; Oh et al., 1999) and Cx43/Cx40 (Valiunas et al., 2000) channels, where this behavior has been attributed to a differential distribution of a fixed charge in the pore of the constituent hemichannels. Rectification of Cx26/Cx32 heterotypic channels was fit well to the Poisson-Nernst-Plank (PNP) model (Suchyna et al., 1999; Oh et al., 1999), which predicts that differences in the specific permeability/selectivity (due to charge distribution across the pore; Chen et al., 1997) properties of constituent hemichannels will result in V_j-dependent charge accumulation or depletion within the channel. Although the PNP model has not been applied in our study, differences in selectivity between Cx46 and Cx50 may explain the modest rectification of the heterotypic Cx46/Cx50. However, independent measurements of selectivity and conductance will be necessary to conclusively evaluate the phenomenon.

Gating of constituent hemichannels in the heterotypic preparation was also significantly altered when compared to the homotypic channels (assuming a positive relative gating polarity for the "main gate" of the constituent hemichannels). At the macroscopic level, comparison of homotypic Cx50 and the assumed Cx50 side of heterotypic junctions shows a clear decrease in the Boltzmann parameter G_{min}. Conversely, the G_{min} of Cx46 was increased in the heterotypic preparation. At the single-channel level transitions to the fully closed state were less frequently observed for heterotypic channels than for homotypic Cx46 channels when V_{j46} was positive. Conversely, transitions to a lower subconductance state and to the fully closed state were more frequently observed when V_{j50} was positive than have been reported for homotypic Cx50 channels (Srinivas et al., 1999). Furthermore, comparison of homotypic Cx46 and heterotypic Cx46/Cx50 at positive V_{j46} values shows a decrease in the frequency of slow gating transitions and an increase in slow gating transitions by the presumed Cx50 side of heterotypic channels compared to homotypic Cx50 (Fig. 7). Taken together, these results argue for the existence of a second gating mechanism in Cx46 channels, with an opposite polarity of voltage sensitivity. Alternatively, the changes in single-channel and macroscopic properties observed when Cx46 and Cx50 are paired may be construed as evidence for a conformational change induced by the docking of the two different hemichannels.

Heteromeric channels

Cx46 and Cx50 are coexpressed in the lens, and immunocytochemical immunopurification techniques indicate that bovine homologs of these two connexins coimmunoprecipitate from lens organ cultures (Jiang and Goodenough, 1996; Konig and Zampighi, 1995). Cx46 and Cx50 have been shown to form functional heteromeric hemichannels by Ebihara et al. (1999) in oocytes; it was therefore of interest to determine the properties of heteromeric Cx46 and Cx50 gap junction channels in mammalian cells. Heteromeric gap junction channels have been shown to be formed by Cx40 and Cx43 (He et al., 1999; Li and Simard, 1999; Elenes et al., 1999), Cx37, and Cx43 (Brink et al., 1997). In both cases, macroscopic and multichannel recordings exhibited properties that were intermediate to those of homotypic junctions, and these intermediate properties were considered as evidence for heteromeric channel formation.

In recordings from Cx46 and Cx50 cotransfected cells, we frequently observed multiple main-state conductance levels (e.g., 115 pS, 164 pS, 158 pS, 180 pS); however, similar channel sizes were often observed in homotypic and heterotypic Cx46 and Cx50 junctions. Heteromeric channel formation was even more difficult to determine from macroscopic recordings because of the similarity of macroscopic properties of homotypic Cx46 and Cx50. The formation of heterotypic channels makes it additionally difficult to unambiguously verify the existence of heteromeric channels from macroscopic recordings. Macroscopic current declines in response to transjunctional voltage in cotransfected cells were not strikingly different from those obtained for Cx46 and Cx50 homotypic and Cx46/Cx50 heterotypic channels. In a few cases, single-channel analysis provided evidence for the heteromerization of Cx46 and Cx50, in that unitary conductances and gating properties were found to differ from either homotypic or heterotypic configurations. However, the low incidence of channels with novel properties leads us to conclude that either heteromeric channel formation is uncommon in N2A cells or that heteromeric channels may not display properties significantly different from those of homotypic and heterotypic channels. Therefore single-channel records that do not show novel properties are not counterindicative of heteromerization. In conclusion, although these studies do not allow an evaluation of the relative affinities of the different connexons for one another or the incidence of connexin mixing within a connexon, they do indicate that the lens connexins are capable of forming functional homomeric, heterotypic, and possibly heteromeric junctional channels. All expression patterns of these connexins investigated in this study led to moderately voltage-sensitive, high-conductance channels that appear to be ideally suited to the exchange of solvent and electrolytes critical for the maintenance of osmotic balance within the transparent lens.

We are grateful to Dr. T.H. Steinberg (Washington University School of Medicine, St. Louis, MO), who provided the Cx46 specific antibody used in these studies; to Dr. Y. Gao, who contributed the immunostaining in Fig. 1; and to Ms. M. Urban, who subcloned Cx46 into the expression plasmid.

This work was supported in part by an AHA Heritage Postdoctoral Fellowship to MS and by a National Institutes of Health grant (EY08969) to DCS.

REFERENCES

Bennett, M. V. L., L. C. Barrio, T. A. Bargiello, D. C. Spray, E. Hertzberg, and J. C. Saez. 1991. Gap junctions: new tools, new answers, new questions. *Neuron.* 6:305–320.

Brink, P. R., K. Cronin, K. Banach, E. Peterson, E. M. Westphale, K. H. Seul, S. V. Ramanan, and E. C. Beyer. 1997. Evidence for heteromeric gap junction channels formed from rat connexin43 and human connexin37. *Am J. Physiol.* 273:C1386–C1396.

Bruzzone, R., T. W. White, and D. L. Paul. 1996. Connections with connexins: the molecular basis of direct intercellular signaling. *Eur. J. Biochem.* 238:1–27.

Bukauskas, F. F., C. Elfgang, K. Willecke, and R. Weingart. 1995. Biophysical properties of gap junction channels formed by mouse connexin40 in induced pairs of transfected human HeLa cells. *Biophys. J.* 68:2289–2298.

Bukauskas, F. F., and R. Weingart. 1994. Voltage-dependent gating of single gap junction channels in an insect cell line. *Biophys. J.* 67:613–625.

Burt, J. M., and D. C. Spray. 1989. Volatile anesthetics reversibly reduce gap junctional conductance between cardiac myocytes. *Circ. Res.* 65: 829–837.

Chen, D., J. Lear, and B. Eisenberg B. 1997. Permeation through an open channel: Poisson-Nernst-Planck theory of a synthetic ionic channel. *Biophys. J.* 72:97–116.

Dermeitzel, R., E. L. Hertzberg, J. A. Kessler, and D. C. Spray. 1991. Gap junctions between cultured astrocytes: immunocytochemical, molecular and electrophysiological analysis. *J. Neurosci.* 11:1421–1432.

Ebihara, L., and E. Steiner. 1993. Properties of a nonjunctional current expressed from a rat connexin46 cDNA in *Xenopus* oocytes. *J. Gen. Physiol.* 102:59–74.

Ebihara, L., X. Xu, C. Oberti, E. C. Beyer, and V. M. Berthoud. 1999. Co-expression of lens fiber connexins modifies hemi-gap-junctional channel behavior. *Biophys. J.* 76:198–206.

Elenes, S., M. Rubart, and A. P. Moreno. 1999. Junctional communication between isolated pairs of canine atrial cells is mediated by homogeneous and heterogeneous gap junction channels. *J. Cardiovasc. Electrophysiol.* 10:990–1004.

Gong, X., G. J. Baldo, N. M. Kumar, N. B. Gilula, and R. T. Mathias. 1998. Gap junctional coupling in lenses lacking alpha3 connexin. *Proc. Natl. Acad. Sci. USA.* 95:15303–15308.

Goodenough, D. A. 1992. The crystalline lens. A system networked by gap junctional intercellular communication. *Semin. Cell Biol.* 3:49–58.

He, D. S., J. X. Jiang, S. M. Taffet, and J. M. Burt. 1999. Formation of heteromeric gap junction channels by connexins 40 and 43 in vascular smooth muscle cells. *Proc. Natl. Acad. Sci. USA.* 96:6495–6500.

Jiang, J. X., and D. A. Goodenough. 1996. Heteromeric connexons in lens gap junction channels. *Proc. Natl. Acad. Sci. USA.* 93:1287–1291.

Konig, N., and G. A. Zampighi. 1995. Purification of bovine lens cell-to-cell channels composed of connexin44 and connexin50. *J. Cell Sci.* 108:3091–3098.

Li, X., and J. M. Simard. 1999. Multiple connexins form gap junction channels in rat basilar artery smooth muscle cells. *Circ. Res.* 84:1277–1284.

Mackay, D., A. Ionides, Z. Kibar, G. Rouleau, V. Berry, A. Moore, A. Shiels, and S. Bhattacharya. 1999. Connexin46 mutations in autosomal dominant congenital cataract. *Am. J. Hum. Genet.* 64:1357–1364.

Mathias, R. T., J. L. Rae, and G. J. Baldo. 1997. Physiological properties of the normal lens. *Physiol. Rev.* 77:21–50.

Moreno, A. P., M. B. Rook, G. I. Fishman, and D. C. Spray. 1994. Gap junction channels: distinct voltage-sensitive and insensitive conductance states. *Biophys. J.* 67:113–119.

Oh, S., J. B. Rubin, M. V. Bennett, V. K. Verselis, and T. A. Bargiello. 1999. Molecular determinants of electrical rectification of single channel conductance in gap junctions formed by connexins 26 and 32. *J. Gen. Physiol.* 114:339–364.

Paul, D. L., L. Ebihara, L. J. Takemoto, K. I. Swenson, and D. A. Goodenough. 1991. Connexin46, a novel lens gap junction protein, induces voltage-gated currents in nonjunctional plasma membrane of *Xenopus* oocytes. *J. Cell. Biol.* 115:1077–1089.

Pfahnl, A., and G. Dahl. 1998. Localization of a voltage gate in connexin46 gap junction hemichannels. *Biophys. J.* 75:2323–2331.

Shiels, A., D. Mackay, A. Ionides, V. Berry, A. Moore, and S. Bhattacharya. 1998. A missense mutation in the human connexin50 gene (GJA8) underlies autosomal dominant "zonular pulverulent" cataract, on chromosome 1q. *Am. J. Hum. Genet.* 62:526–532.

Spray, D. C., A. L. Harris, and M. V. L. Bennett. 1981. Equilibrium properties of a voltage-dependent junctional conductance. *J. Gen. Physiol.* 77:75–94.

Srinivas, M., M. Costa, Y. Gao, A. Fort, G. I. Fishman, and D. C. Spray. 1999. Voltage dependence of macroscopic and unitary currents of gap junction channels formed by mouse connexin50 expressed in rat neuroblastoma cells. *J. Physiol. (Lond.).* 517:673–689.

Steele, E. C., Jr., M. F. Lyon, P. H. Glenister, P. Guillot, and R. L. Church. 1997. Identification of a mutation in the connexin50 (Cx50) gene of the No2 cataractous mouse mutant. *In* Gap Junctions. R. Werner, editor. IOS Press, Amsterdam. 289–293.

Suchyna, T. M., J. M. Nitsche, M. Chilton, M., A. L. Harris, R. D. Veenstra, and B. J. Nicholson. 1999. Different ionic selectivities for connexins 26 and 32 produce rectifying gap junction channels. *Biophys. J.* 77:2968–2987.

Trexler, E. D., M. V. L. Bennett, T. A. Bargiello, and V. K. Verselis. 1996. Voltage gating and permeation in a gap junction hemichannel. *Proc. Natl. Acad. Sci. USA.* 93:5836–5841.

Unger, V. M., N. M. Kumar, N. B. Gilula, and M. Yeager. 1999. Three-dimensional structure of a recombinant gap junction membrane channel. *Science.* 283:1176–1180.

Valiunas, V., R. Weingart, and P. R. Brink. 2000. Formation of heterotypic gap junction channels by connexins 40 and 43. *Circ. Res.* 86:42–49.

Veensta, R. D., and R. L. DeHaan. 1988. Cardiac gap junction activity in embryonic chick ventricle cells. *Am J. Physiol.* 254:H170–H180.

Verselis, V. K., C. S. Ginter, and T. A. Bargiello. 1994. Opposite voltage gating polarities of two closely related connexins. *Nature.* 368:348–351.

Verselis, V. K., and R. D. Veenstra. 2000. Gap junction channels: permeability and voltage gating. *In* Advances in Molecular and Cell Biology. Edward Bittar and Elliot Hertzberg, editors. JAI Press, Stanford, CT. 129–192.

White, T. W., R. Bruzzone, D. A. Goodenough, and D. L. Paul. 1992. Mouse Cx50, a functional member of the connexin family of gap junction proteins, is the lens fiber protein MP70. *Mol. Biol. Cell.* 3:711–720.

White, T. W., R. Bruzzone, D. A. Goodenough, and D. L. Paul. 1994a. Voltage gating of connexins. *Nature.* 371:208–209.

White, T. W., R. Bruzzone, S. Wolfram, D. L. Paul, and D. A. Goodenough. 1994b. Selective interactions among the multiple connexin proteins expressed in the vertebrate lens: the second extracellular domain is a determinant of compatibility between connexins. *J. Cell Biol.* 125:879–892.

White, T. W., D. L. Paul, and D. A. Goodenough. 1998. Targeted ablation of connexin50 in mice results in microphthalmia and zonular pulverulent cataracts. *J. Cell Biol.* 143:815–825.

Wilders, R., and H. J. Jongsma. 1992. Limitations of the dual voltage clamp method in assaying conductance and kinetics of gap junction channels. *Biophys. J.* 63:942–953.